International Atomic Energy Agency

INDC(CCP)-316
Distr. L

INDC INTERNATIONAL NUCLEAR DATA COMMITTEE

EVALUATED NEUTRON NUCLEAR DATA

FOR CURIUM-244

A.B. Klepatskij, A.M. Kolesov, V.M. Maslov
Yu.V. Porodzinskij, E.Sh. Sukhovitskij

Academy of Sciences of the Byelorussion SSR
Institute of Nuclear Energetics

Minsk 1989

INDC(CCP)-316
Distr. L

EVALUATED NEUTRON NUCLEAR DATA

FOR CURIUM-244

A.B. Klepatskij, A.M. Kolesov, V.M. Maslov
Yu.V. Porodzinskij, E.Sh. Sukhovitskij

Academy of Sciences of the Byelorussion SSR
Institute of Nuclear Energetics

Minsk 1989

English translation of an unnumbered report
labelled "Preprint No. I", Minsk 1989

ABSTRACT

The creation of an evaluated neutron data file for ^{244}Cm is described. Currently available information on the interaction of neutrons with the ^{244}Cm nucleus is analysed. Owing to a lack of experimental data the evaluation relies to a large extent on the use of theoretical models and systematics. The evaluated cross-sections obtained in the 10^{-5} eV - 20 MeV region are compared with evaluations made by other authors.

Reproduced by the IAEA in Austria
October 1991

91-05732

CONTENTS

EVALUATED NEUTRON NUCLEAR DATA FOR CURIUM-244

INTRODUCTION

The ^{244}Cm nucleus is a strong α-emitter with a half-life of (18.11 ± 0.02) a and, consequently, it is a powerful heat source. Thus, ^{244}Cm is responsible for almost 50% of the total thermal emission level in spent fuel after a three-year cooling period. The isotope ^{244}Cm is formed by irradiation in the neutron beam of the reactor:

$$\left.\begin{matrix}^{242}\mathrm{Am} \\ ^{242}\mathrm{Am}\end{matrix}\right\rangle \xrightarrow{n,\gamma} {}^{243}\mathrm{Am} \xrightarrow{n,\gamma} {}^{244}\mathrm{Am} \xrightarrow{\beta^-} {}^{244}\mathrm{Cm} \ .$$

The spontaneous fission life of ^{244}Cm is $(1.344 \pm 0.002)\cdot 10^7$ a ($\bar{\nu}_{c.\Delta} = 2.690 \pm 0.008$).

The accuracy level required at present in ^{244}Cm accumulation calculations (these requirements stem from processing and transport contingencies) is ~ 30%; therefore, the fission and radiative capture cross-sections for ^{244}Cm must be determined to an accuracy of 10-30% over a wide energy range [1]. However, the differences between the evaluated cross-sections for the (n,f) and (n,γ) reactions given in the JENDL-2 and ENDF/B libraries can be as high as 100% [1]. These discrepancies have served as a stimulus for this current evaluation.

This paper describes the results of an evaluation of all ^{244}Cm neutron cross-section types in the 10^{-5} eV - 20 MeV energy region. In view of the limited quantity of experimental data available on ^{244}Cm neutron cross-sections, the evaluation was based in the main on theoretical models and known parameter systematics.

Table 1 shows the energies Q and thresholds T for various reactions of neutrons with a ^{244}Cm nucleus. The threshold value (for negative values of Q) was obtained using the expression

$$T = \frac{M_n + M_{244}}{M_{244}}(-Q) = \frac{1,0086652 + 244,062763}{244,062763}(-Q) =$$

$$= 1,004132\,(-Q) \ ,$$

where Mn is the neutron mass and M244 is the mass of the ^{244}Cm nucleus.

Owing to the Coulomb barrier, the cross-sections of reactions with emission of charged particles are so small as to be negligible in the energy region under consideration, and we therefore did not evaluate them.

The ^{244}Cm level system was studied up to ~ 2 MeV (Table 2).

Above 500 keV there are quite probably undiscovered levels, and for that reason only the first five levels in Table 2 were used in the evaluation.

Table 1

Energy (Q) and threshold (T) values for reactions of neutrons with the ^{244}Cm nucleus, MeV

Reaction	Q	T
$(n,\gamma)^{245}Cm$	5,519	-5,519
$(n,2n)^{245}Cm$	-6,799	6,827
$(n,3n)^{242}Cm$	-12,500	12,552
$(n,4n)^{241}Cm$	-19,469	19,549
$(n,p)^{244}Am$	-0,647	0,65
$(n,np)^{243}Am$	-6,015	6,04
$(n,d)^{243}Am$	-3,784	3,80
$(n,t)^{242}Am$	-3,904	3,92
$(n,^{3}He)^{242}Pu$	-3,137	3,15
$(n,^{4}He)^{241}Pu$	11,14	-11,14

Table 2

^{244}Cm level system [2]

Level No.	Level energy, keV	Spin, parity	Level No.	Level energy, keV	Spin, parity
1	0,0	0^+	6	970	$(2^+, 3^-)$
2	42,9	2^+	7	1038	$(2^+, 3^-)$
3	142,3	4^+	8	1042	6^+
4	296	6^+	9	1187	$(2^+, 3^-)$
5	502	8^+	10	2000	-

1. NEUTRON CROSS-SECTIONS FOR ^{244}Cm IN THE RESOLVED RESONANCE REGION

1.1. Experimental data for ^{244}Cm in the resolved resonance region

For the evaluation we used data from the following experimental work:

1. Cote et al., [3] measured the total cross-section in the 0.01-900 eV region. Owing to poor resolution, neutron widths were obtained for resonances up to 300 eV but the shape and distribution of total widths were analysed for only three resonances. The mean radiation width obtained by the authors for these three resonances - (37.5 ± 1.2) meV - includes a fission width which is not specified;

2. Berreth et al., [4] measured the total cross-section of ^{244}Cm up to 90 eV and determined the neutron widths by analysing areas, assuming that $\Gamma_\gamma + \Gamma_f = 40$ meV. A total width was only obtained for the first resonance;

3. Simpson et al., [5] measured transmission in ^{244}Cm samples $1212 \cdot 10^{-28}$ m^2/atom thick in the 6-530 eV region. The resonance parameters they give were obtained by joint analysis of their own experiments and data from Refs [3,4,6];

4. Moore and Keyworth [6] measured the capture and fission cross-sections over a wide energy range with high resolution using neutrons from a nuclear explosion, and were thus able to obtain resonance parameters for the 20-1000 eV region by analysing areas assuming the constant width Γ_γ=37 meV;

5. Belanova et al., [7] measured the total cross-sections for ^{244}Cm using the time-of-flight method, and determined the neutron and total widths of the first four resonances at energies up to 220 eV using the shape and areas method;

6. Maguire, et al., [8] measured the fission cross-section in the 0.1 eV - 80 keV region and determined the areas under the first four fission resonances.

Apart from the above work, measurements have also been taken of ^{244}Cm neutron cross-sections at thermal energy level, resonance integrals (Table 1.1), and the coherent scattering amplitude $b_{coh} = (095 \pm 0.03) \cdot 10^{-14}$ m [16].

Table 1.1

Thermal cross-sections and resonance integrals for ^{244}Cm, 10^{-28} m^2

Ref.	σ_t	σ_{nf}	$\sigma_{n\gamma}$	I_f	I_γ
[10]	-	1 ± 1	-	-	-
[11]	-	-	-	-	650 ± 50
[12]	-	1,5 ± 1,0	14 ± 4	12,5 ± 2,5	650 ± 50
[4]	23 ± 3	-	-	-	-
[13]	-	1,1 ± 0,3	-	18 ± 1	-
[9]	-	-	25 ± 10	-	-
[14]	-	1,0 ± 0,2	-	13,4 ± 1,5	-
[15]	-	-	15,2 ± 1,2	-	626 ± 53
Our evaluation	27,63 ± 1,37	1,03 ± 0,18	15,26 ± 1,14	-	-

1.2. Evaluated resonance parameters

During the first stage, the mean radiation width of the first three resonances Γ_γ = (35 ± 1.2) meV was obtained using the measured total widths from Refs. [3,7] and fission width from Ref. [8]. This value tallies with the capture width value of (37.5 ± 1.2) meV obtained in Ref. [3], which includes the mean fission width for these three resonances (~ 1.6 meV). Then, the neutron widths of resonances with energies over 20 eV were determined from the areas under the fission and capture resonances given in Ref. [6]. It was assumed that the radiation width was (35 ± 6) meV, and the error level covers dispersion of the mean value. The error levels for the values of Γ_n obtained take into account uncertainties with regard to the areas and radiative capture widths.

The neutron widths obtained in this way were averaged with widths from other sources. The values of Γ_n obtained were assumed to be evaluated. Together with the areas under the capture and fission resonances from Ref. [6] they define in full the resonance parameters. However, owing to the direct computation method used for certain resonances, anomalous radiative capture width values were produced at variance with their known limited fluctuation. In order to avoid this, we used the method of least squares to minimize

deviations (in dispersion units) in the areas under resonance and radiation widths from the mean value. This procedure significantly reduces fluctuation of the evaluated radiation widths.

Table 1.2 gives the evaluated resonance parameters for ^{244}Cm. The parameters of the negative resonance are selected in such a way as to describe the evaluated cross-sections at the thermal point.

Table 1.2

Evaluated resonance parameters for ^{244}Cm, meV

E_r, eV	Γ_n	Γ_f	Γ_γ
1	2	3	4
-17,28	47,63	6,17	36,0
7,67	1,01	0,12	35,1
16,77	1,95	1,4	35,1
22,85	0,89	3,34	33,4
34,99	3,51	2,25	33,3
52,78	0,55	1,65	35,6
69,99	0,67	2,83	35,2
85,96	25,47	0,63	35,9
96,12	7,26	1,51	36,2
132,8	13,49	1,32	41,3
139,1	2,49	2,74	35,6
171,2	3,21	1,23	35,9
181,6	9,56	2,16	37,8
197,0	32,97	1,17	43,4
209,8	44,49	0,48	34,7
222,1	40,88	1,34	39,1
230,5	30,32	0,38	35,0
234,9	3,92	0,87	34,8
242,7	1,35	3,67	35,0
264,9	11,3	0.86	34,3
274,1	21,25	0,54	31,9
361,8	5,63	0,28	34,4
329,5	42,57	0,34	42,9
343,6	41,89	0,9	28,5
353,1	117,39	1,21	34,7
361,7	23,41	1,17	41,7
364,4	10,1	1,98	35,0
386,2	26,21	1,07	35,2
397,6	19,61	0,74	41,4
415,0	20,38	0,24	33,1
420,6	122,76	0,82	33,5
426,9	14,8	0,31	32,2
443,4	67,79	0,87	38,6
470,9	85,94	2,08	41,6
488,9	15,97	0,45	33,2
491,9	60,88	0,43	33,8
512,4	122,9	0,25	45,3
520,5	33,85	2,06	29,9

1.3. Mean resonance parameters in the resolved resonance region

The mean inter-level distances <D> and the mean neutron width $\langle\Gamma_n^o\rangle$ were evaluated using the methodology in Ref. [17]: <D> = (11.0 ± 0.83) eV, $\langle\Gamma_n^o\rangle$ = (1.34 ± 0.31) $meV^{1/2}$. The error levels here are mainly due to the finiteness of the selected set of evaluated resonances. The mean radiation width $\langle\Gamma_\gamma\rangle$ = (36.04 ± 6) meV and the number of degrees of freedom for distribution of the widths Γ_γ, calculated using the formula

$$\nu_\Gamma = \frac{2\langle\Gamma_\Gamma\rangle^2}{\langle\Gamma_\Gamma^2\rangle - \langle\Gamma_\Gamma\rangle^2}$$

was 180.

The mean fission width is (1.23 ± 0.35) meV. The error level for the evaluated value of $\langle\Gamma_f\rangle$ was due to normalization and the finiteness of the selected set.

Comparing the mean resonance parameters obtained with the evaluation given in ENDF/B-V (<D> = 14.1 meV, $\langle\Gamma_n^o\rangle$ = 1.695 $meV^{1/2}$, $\langle\Gamma_\gamma\rangle$ = 36.24 meV, $\langle\Gamma_f\rangle$ = 1.35 meV), we see that the fission and radiation widths and the strength function S_0 tally. The differences in the values of <D> are probably due to the fact that we allow for a ~ 25% level omission in our evaluation.

2. NEUTRON CROSS-SECTIONS IN THE UNRESOLVED RESONANCE REGION

In our evaluation, the unresolved resonance region was limited to the 0.5-43 keV energy range. The lower level corresponds to the upper limit of the resolved resonance region, and the upper level to the inelastic scattering reaction threshold. We chose this range because experimental data in this region were not accurate enough, and because we had no accurate knowledge of the strength function S_2.

2.1. Experimental data in the unresolved resonance region

In this region there are data available on the total cross-section within the narrow energy range of 0.5-0.8 keV [3], and on the fission cross-section [6,8] and the radiative capture cross-section for energies up to 9 keV [6]. Table 2.1 shows the values given in these sources averaged over the intervals.

Table 2.1

Experimental data in the unresolved resonance region, 10^{-28} m^2

E, keV	$\langle\sigma_t\rangle$ [3]	$\langle\sigma_f\rangle$ [6]	$\langle\sigma_f\rangle$ [8]	$\langle\sigma_\gamma\rangle$ [6]
0,5-0,6	31,73	0,240	0,438	13,58
0,6-0,7	35,26	0,274	0,422	18,40
0,7-0,8	27,78	0,271	0,471	10,45
0,8-1,0		0,310	0,429	8,37
1,0-1,2		0,092	0,304	7,96
1,2-1,4		0,121	0,239	12,49
1,4-1,6		0,130	0,235	8,94
1,6-2,0		0,167	0,248	5,81
2,0-2,4		0,114	0,197	4,32
2,4-2,8		0,109	0,172	4,19
2,8-3,2		0,116	0,166	3,69
3,2-3,6		0,107	-	1,77
3,6-4,0		0,105	0,155	1,50
4,0-4,5		0,111	0,148	3,50
4,5-5,0		0,080	0,131	3,55
5,0-6,0		0,101	0,142	3,27
6,0-7,0		0,113	0,119	3,01
7,0-8,0		0,090	0,127	1,11
8,0-10,0		0,094	0,113	1,42
10-12		0,086	0,111	
12-14		0,064	0,100	
14-16		0,063	0,104	
16-20		0,082	0,094	
20-24		0,083	0,080	
24-28		0,058	0,077	
28-32		0,074	0,069	
32-36		0,087	0,067	
36-40		0,062	0,063	
40-45		0,055	0,064	

2.2. Evaluated mean resonance parameters

The mean inter-level distances and the neutron widths were obtained using the generally accepted methodology from the value of <D> evaluated in the resolved resonance region and the strength functions S_0, S_1, S_2. The strength function $S_0 = 1.218 \cdot 10^{-4} (eV)^{-1/2}$ was taken from the resolved resonance region, with an energy dependence which may be calculated using the generalized optical model employing the potential parameters described in Section 4: $S_0 = 1.218$ ($E_n = 0.1$ keV); $S_0 = 1.126$ ($E_n = 20$ keV); $S_0 = 1.103$ ($E_n = 40$ keV). The strength function $S_1 = 3.3 \cdot 10^{-4} (eV)^{-1/2}$ was obtained using the same calculations; S_2 was assumed to be equal to S_0

Table 2.2

Evaluated mean inter-level distances for the ^{245}Cm compound nucleus, eV

E*, keV	<D>**$_{1/2}$	<D>**$_{3/2}$	<D>**$_{5/2}$
0,55	10,99	5,70	4,04
0,65	10,98	5,70	4,04
0,75	10,98	5,70	4,04
0,90	10,98	5,70	4,04
1,1	10,97	5,69	4,04
1,3	10,97	5,69	4,04
1,5	10,97	5,69	4,03
1,8	10,96	5,69	4,03
2,2	10,95	5,68	4,03
2,6	10,94	5,68	4,03
3,0	10,93	5,67	4,02
3,4	10,92	5,67	4,02
3,8	10,92	5,66	4,02
4,25	10,91	5,66	4,01
4,75	10,90	5,65	4,01
5,5	10,88	5,64	4,00
6,5	10,86	5,63	4,00
7,5	10,83	5,62	3,99
9,0	10,80	5,60	3,97
11	10,76	5,58	3,96
13	10,72	5,56	3,94
15	10,67	5,54	3,93
18	10,61	5,50	3,90
22	10,52	5,46	3,87
26	10,44	5,42	3,84
30	10,36	5,37	3,81
34	10,28	5,33	3,78
38	10,19	5,29	3,75
42,5	10,10	5,24	3,71

* Energy counted from the neutron binding energy

** It is assumed that the inter-level distance is not dependent on parity.

with no energy dependence. The evaluated mean inter-level distances and mean neutron widths are given in Tables 2.2 and 2.3.

The anomalously high fission widths given in Ref. [6] for the compound nucleus ^{245}Cm around 820 keV may be caused by the second hump in the fission barrier. However, experimental data on charged particle-induced fission [18] and fission barrier systematics [19] show that the second fission barrier hump for ^{245}Cm is below the neutron binding energy and has practically no

influence on the value and distribution of fission widths. Therefore, the mean fission widths were evaluated using the single hump barrier in the Hill-Wheeler model.

Table 2.3

Evaluated mean neutron widths for ^{244}Cm, meV

E, keV	$\langle\Gamma^0_n\rangle_{1/2^+}$	$\langle\Gamma^1_n\rangle_{1/2^-}$	$\langle\Gamma^1_n\rangle_{3/2^-}$	$\langle\Gamma^2_n\rangle_{3/2^+}$	$\langle\Gamma^2_n\rangle_{5/2^+}$
0,55	31,33	0,16	0,08	0,0	0,0
0,65	34,04	0,21	0,11	0,0	0,0
0,75	36,55	0,25	0,13		
0,90	40,00	0,34	0,18		
1,1	44,17	0,46	0,24		
1,3	47,96	0,59	0,30		
1,5	51,46	0,72	0,38		
1,8	56,27	0,95	0,49		
2,2	62,07	1,28	0,67		
2,6	67,32	1,64	0,85		
3,0	72,14	2,03	1,05		
3,4	76,62	2,45	1,27		
3,8	80,81	2,89	1,50		
4,25	85,24	3,41	1,77		
4,75	89,85	4,01	2,08		
5,5	96,26	4,98	2,58		
6,5	104,03	6,36	3,30		
7,5	111,09	7,84	4,07		
9,0	120,61	10,23	5,31		
11	131,77	13,67	7,09	0,01	0,01
13	141,55	17,38	9,02	0,02	0,01
15	150,23	21,31	11,06	0,02	0,02
18	161,61	27,58	14,31	0,04	0,03
22	175,47	36,49	18,93	0,06	0,04
26	188,53	45,92	23,82	0,09	0,07
30	200,15	55,75	28,92	0,13	0,09
34	210,59	65,90	34,19	0,18	0,13
38	220,03	76,30	39,58	0,23	0,16
42,5	229,74	88,22	45,77	0,30	0,21

The fission barrier threshold E_f = 6.22 was taken from Refs.[6,18,19]. The curvature $\hbar\omega$ = 0.553 MeV was determined using the mean fission width in the resolved resonance region. The number of fission channels φ_f was assumed to be 2J + 1.

Figure 2.1 compares the fission cross-sections calculated using the above parameters and experimental data from Ref. [6]. Clearly, above 4 keV the calculated cross-sections are systematically lower than the experimental ones.

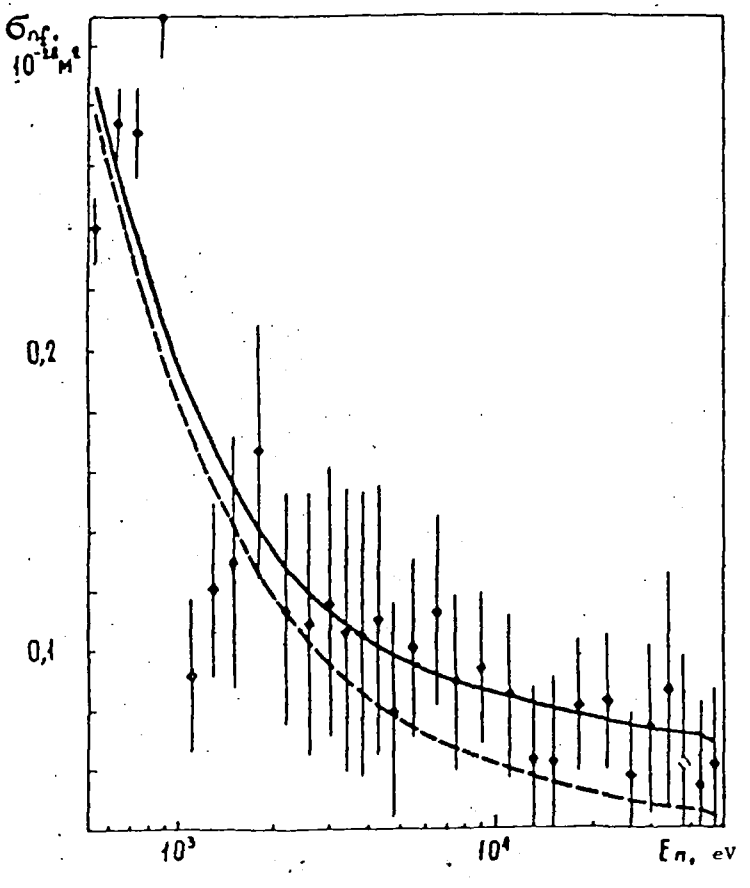

Fig. 2.1 Comparison of experimental [6] and calculated data on σ_{nf} (^{244}Cm) in the 0.5-4.3 keV region: - - - fission barriers from Refs. [6,8,9]; _____ after barrier correction

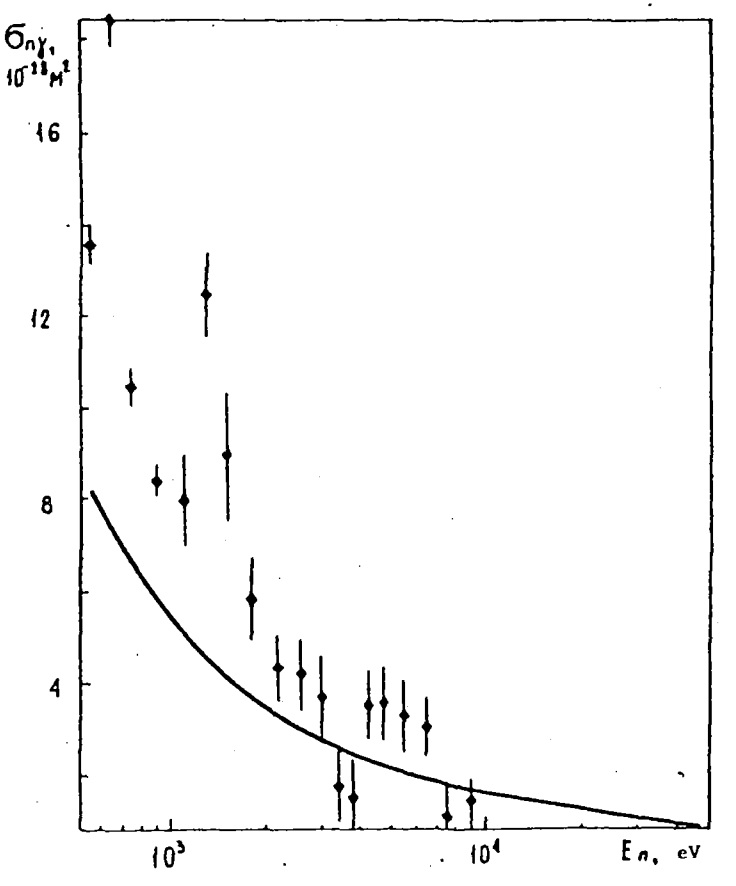

Fig. 2.2 Comparison of calculated and experimental [6] radiative capture cross-sections in the 0.5-43 keV region.

In order to make them tally on average, the fission thresholds for states which may be formed by $\ell = 1$ neutrons were lowered by 50 keV. As may be seen from the figure, this set of fission barrier parameters makes for an almost total agreement between the experimental and calculated cross-sections for energies above 2 keV. At lower energy levels, the calculated curve, while it fits the experimental data on average, does not reproduce the measured structure of the cross-sections. Therefore, in the 0.5-2 keV region the evaluated mean fission widths in the $\ell = 0$ channel were obtained by fitting the calculated cross-sections to the experimental ones.

The evaluated values for the mean fission widths are given in Table 2.4.

Table 2.4

Evaluated mean fission widths, meV

E, keV	$\langle\Gamma^{0}_{f\,1/2}\rangle^{+}$	$\langle\Gamma^{1}_{f\,1/2}\rangle^{-}$	$\langle\Gamma^{1}_{f\,3/2}\rangle^{-}$	$\langle\Gamma^{2}_{f\,3/2}\rangle^{+}$	$\langle\Gamma^{2}_{f\,5/2}\rangle^{+}$
0,55	1,03	2,18	2,26	1,28	1,36
0,65	1,35	2,18	2,26	1,28	1,36
0,75	1,48	2,18	2,26	1,28	1,36
0,90	1,98	2,19	2,27	1,29	1,37
1,1	0,51	2,19	2,27	1,29	1,37
1,3	0,84	2,19	2,27	1,29	1,37
1,5	1,01	2,20	2,28	1,29	1,37
1,8	1,59	2,20	2,28	1,30	1,38
2,2	1,25	2,21	2,29	1,30	1,38
2,6	1,26	2,22	2,30	1,31	1,39
3,0	1,26	2,23	2,31	1,31	1,39
3,4	1,27	2,24	2,32	1,32	1,40
3,8	1,27	2,25	2,33	1,32	1,40
4,25	1,28	2,26	2,34	1,33	1,41
4,75	1,29	2,27	2,35	1,33	1,42
5,5	1,29	2,28	2,37	1,34	1,43
6,5	1,31	2,30	2,39	1,35	1,44
7,5	1,32	2,33	2,41	1,37	1,45
9,0	1,34	2,36	2,44	1,39	1,47
11	1,36	2,40	2,49	1,41	1,50
13	1,39	2,45	2,54	1,44	1,53
15	1,41	2,49	2,58	1,47	1,56
18	1,45	2,56	2,66	1,51	1,60
22	1,51	2,66	2,76	1,57	1,66
26	1,57	2,76	2,86	1,62	1,73
30	1,63	2,87	2,97	1,69	1,79
34	1,69	2,98	3,08	1,75	1,86
38	1,75	3,09	3,20	1,83	1,93
42,5	1,83	3,22	3,34	1,90	2,01

The mean radiation width was calculated using the gamma-ray emission cascade theory, and its absolute value was normalized to the mean value from the resolved resonance region (Table 2.5). Dependence of $\langle\Gamma_\gamma\rangle$ on parity was not taken into account.

Comparing of the radiative capture cross-sections calculated using the above widths with the experimental data from Ref. [6], we see (Fig. 2.2) that below 2 keV the calculated cross-sections are significantly lower than the experimental ones. Any reasonable change in the parameters for the s-wave (the contribution of the remaining partial waves in this region is so small as to be negligible) fails to produce agreement. We therefore feel there must be

Table 2.5

Evaluated mean radiation widths, meV

E,keV	$\langle\Gamma_\gamma\rangle_{1/2}$	$\langle\Gamma_\gamma\rangle_{3/2}$	$\langle\Gamma_\gamma\rangle_{5/2}$	E, keV	$\langle\Gamma_\gamma\rangle_{1/2}$	$\langle\Gamma_\gamma\rangle_{3/2}$	$\langle\Gamma_\gamma\rangle_{5/2}$
0,55	36,05	35,66	35,02	4,75	36,12	35,73	35,09
0,65	36,05	35,66	35,02	5,5	36,14	35,75	35,11
0,75	36,05	35,66	35,03	6,5	36,15	35,76	35,12
0,90	36,06	35,67	35,03	7,5	36,17	35,78	35,14
1,1	36,06	35,67	35,03	9,0	36,20	35,81	35,17
1,3	36,06	35,67	35,04	11	36,23	35,84	35,20
1,5	36,07	35,68	35,04	13	36,27	35,88	35,24
1,8	36,07	35,68	35,04	15	36,30	35,91	35,27
2,2	36,08	35,69	35,05	18	36,35	35,96	35,32
				22	36,42	36,03	35,39
2,6	36,09	35,69	35,06	26	36,50	36,10	35,46
3,0	36,09	35,07	35,06	30	36,57	36,17	35,53
3,4	36,10	35,71	36,07	34	36,61	36,24	35,60
3,8	36,11	35,72	35,08	38	36,71	36,31	35,67
4,25	36,11	35,72	35,09	42,5	36,79	36,39	35,75

Table 2.6

Number of degrees of freedom of the χ^2-distribution of mean partial widths

ℓ	J	π	ν_n	ν_f	ν_γ
0	1/2	+	1	2	
1	1/2	-	1	2	
1	3/2	-	1	4	∞
2	3/2	+	1	4	
2	5/2	+	1	6	

some kind of unrecognized error in the experimental data on $\sigma_{n\gamma}$ given in Ref. [6], and we view the calculated cross-sections as being evaluated. Table 2.6 gives the numbers of degrees of freedom of the χ^2-distribution of the widths required to calculate the evaluated cross-sections in the unresolved resonance region.

3. FISSION CROSS-SECTION FOR ^{244}Cm IN THE FAST NEUTRON REGION (0.043-20 MeV)

Measurement of ^{244}Cm fission cross-sections is difficult owing to the high α-activity of this isotope. As a result, few experimental data are available on $\sigma_{nf}(^{244}Cm)$, they all have a fairly wide spread, and cover a small energy interval up to ~ 4 MeV.

3.1. Experimental data on $\sigma_{nf}(^{244}Cm)$ in the fast neutron region

The following experimental data were used in the evaluation:

1. Moore and Keyworth [6] determined the ratio of the ^{244}Cm fission cross-section to the ^{235}U fission cross-section up to ~ 3 MeV with good resolution and to an accuracy of ~ 8%;

2. Fomushkin, et al., [19] measured the $\sigma_{nf}(^{244}Cm)/\sigma_{nf}(^{235}U)$ ratio in the 0.3-4 MeV region to an accuracy of ~ 5% above the threshold. The $\sigma_{nf}(^{244}Cm)$ curve was absolutized to an accuracy of ~ 6% using the integral $\int\sigma_f(E)_f(E)dE$ [20];

3. Koontz and Barton [21] determined the $\sigma_{nf}(^{244}Cm)/\sigma_{nf}(^{235}U)$ ratio at four energy points (1, 1.5, 3 and 14.9 MeV). As this was only a preliminary publication, the authors did not give the error levels for their measurements. However, no further information appeared subsequently and therefore the error levels they obtained in the same experiment for ^{238}Pu have been applied to the data in Ref. [21];

4. Vorotnikov, et al., [22] measured $\sigma_{nf}(^{244}Cm)$ in the 0.39-1.3 MeV region with an error level of ~ 15-20%;

5. Fomushkin, et al., [23] determined the $\sigma_{nf}(^{244}Cm)/\sigma_{nf}(^{238}U)$ ratio at 14.5 MeV using two methods, glasses and a fission chamber, with an error level of ~ 10%.

3.2. Evaluation of the fission cross-section for ^{244}Cm

The measured $\sigma_{nf}(^{244}Cm)/\sigma_{nf}(^{235}U)$ and $\sigma_{nf}(^{244}Cm)/\sigma_{nf}(^{238}U)$ ratios were converted into absolute cross-sections using the σ_{nf} values for ^{235}U given in Ref. [24] and the σ_{nf} value for ^{238}U given in Ref. [25] as a standard (Figs. 3.1-3.3).

As mentioned above, the experimental results cover the region up to the threshold of the (n,n'f) reaction. Looking at Figs. 3.1 and 3.2, we see that the data from the various sources do not contradict one another, if one allows for the fact that the energies of the experimental points in Ref. [19] should be reduced by 100 keV, and the two last points in Ref. [22] are wrong. Using the method of least squares, and taking into account measurement errors, the $\sigma_{nf}(E)$ curve for the 0.043-4 MeV region was drawn through the experimental points.

Above 4 MeV there are no data on the neutron-induced fission cross-section for ^{244}Cm except for the measurement in Ref. [23] at 14.5 MeV and the one in Ref. [21] at 14.9 MeV. However, the high cross-section values given in Ref. [23] are difficult to interpret since they are higher than the evaluated cross-section for formation of the compound nucleus. Therefore, the evaluated $\sigma_{nf}(E)$ curve for this region was obtained by calculation using the statistical cascade theory; it was assumed that the proportion of pre-equilibirum emission in the spectrum of the first neutron, as calculated for uranium isotopes in Ref. [26], changes insignificantly from nucleus to nucleus. The fission barrier parameters for the compound nuclei ^{244}Cm and ^{243}Cm, which fission in the (n,n'f) and (n,2nf) reactions, were selected in the light of the data on charged particle-induced fission contained in Ref. [27]. The neutron transmission coefficients needed for the calculations were calculated using the generalized optical model with potential parameters (selection of the latter is described in Section 4).

The evaluated fission cross-section values are compared with the evaluation given in ENDF/B-V [28] and experimental data in Figs. 3.1-3.3, and the evaluated $\sigma_{nf}(^{244}Cm)/\sigma_{nf}(^{235}U)$ ratio is shown in Table 3.1. Below 4 MeV the error levels reflect the spread of the experimental data; above that level they reflect the predicted accuracy of the calculation.

Our evaluation is practically identical with the evaluation given in ENDF/B-V up to ~ 1 MeV. In the 1-4 MeV range, the differences between the

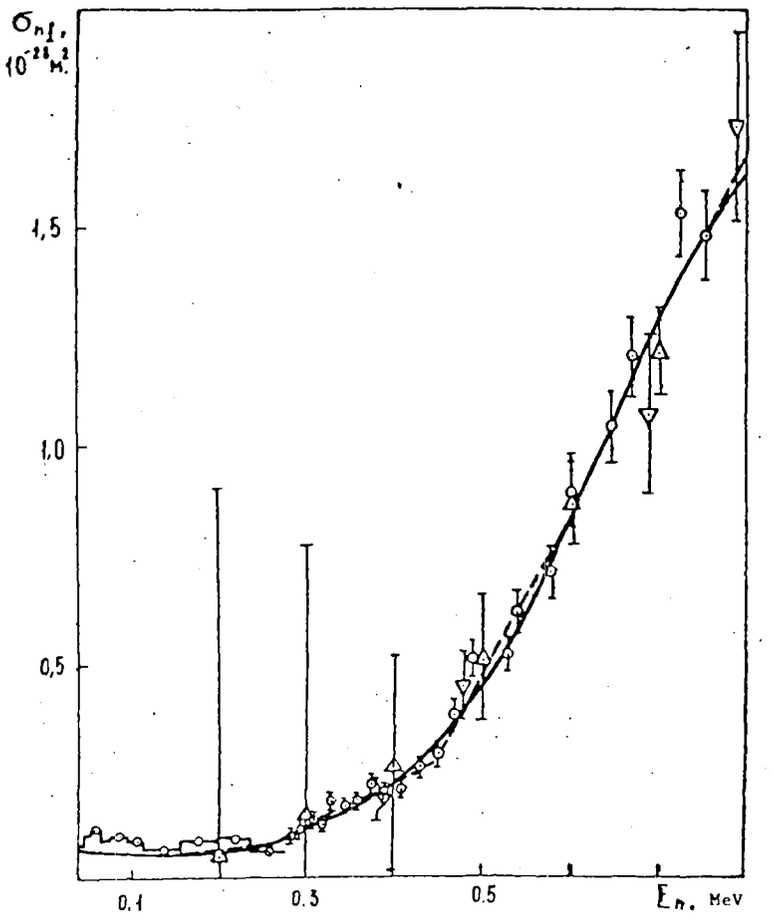

Fig. 3.1. Comparison of evaluated data on σ_{nf} up to 0.8 MeV:
- /6/; - /19/; - /21/; - /22/; —— Our evaluation;
- - - Evaluation is ENDF/B - V /28/

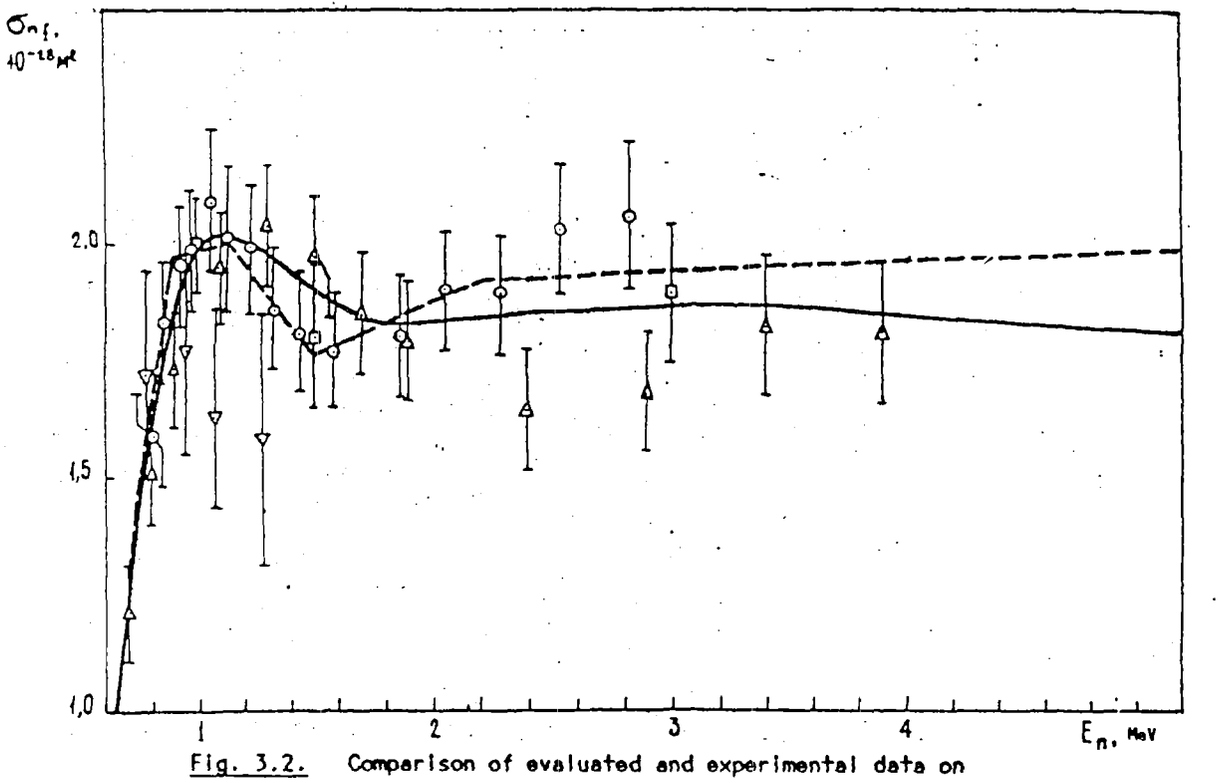

Fig. 3.2. Comparison of evaluated and experimental data on σ_{nf} in the 0.7-5 MeV region (see key to Fig. 3.1)

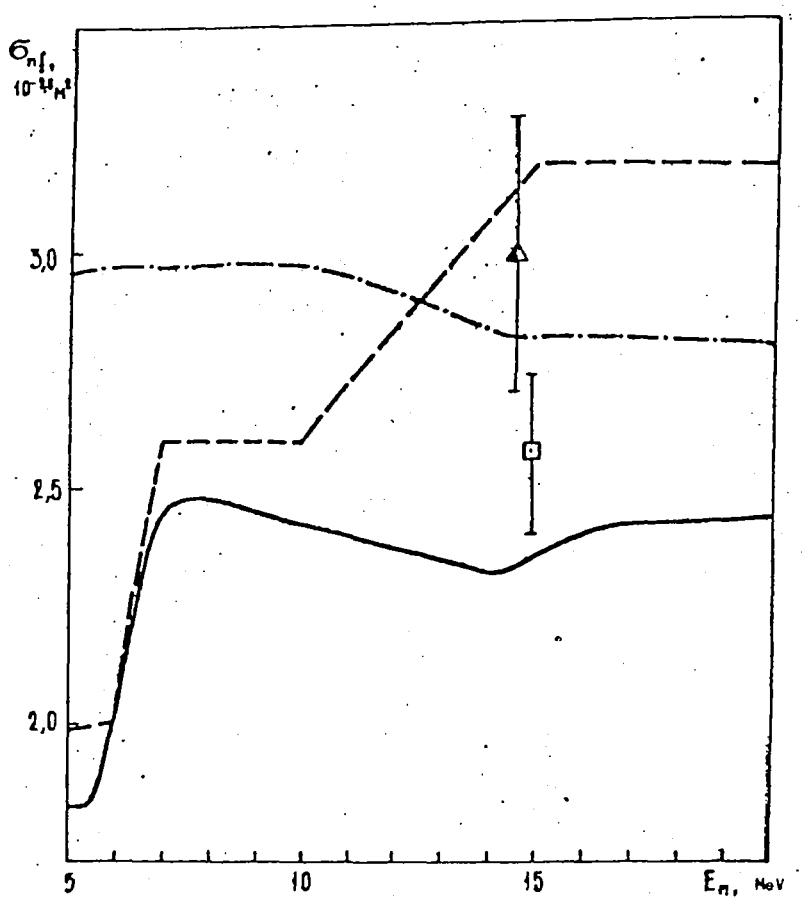

Fig. 3.3. Comparison of experimental and evaluated data on σ_{nf} in the 5-20 MeV region ⊥ - [23]; —.—.— - calculated cross-section for formation of the compound nucleus (for rest see Fig. 3.1)

two sources amount to 5-7%. This is probably due to the fact that the evaluation in Ref. [28] is based on data from Ref. [6], published in 1971, and we took into account the more recent experimental results published in Ref. [19]. The greatest differences between the two evaluations occur above the threshold of the (n,2nf) reaction and amount to $0.7 \cdot 10^{-28}$ m^2. The evaluated cross-section value for σ_{nf} given in Ref. [28] for this region is clearly an overestimate since it is higher even than the cross-section for formation of the compound nucleus as predicted by the generalized optical model (Fig. 3.3).

4. CROSS-SECTIONS FOR INTERACTION OF FAST NEUTRONS WITH THE ^{244}Cm NUCLEUS

Apart from the fission cross-section measurements described in the previous section, no experimental data are available on the cross-sections for interaction of neutrons with the ^{244}Cm nucleus in the 0.043-20 MeV region.

Table 3.1

Evaluated $\sigma_{nf}(^{244}Cm)/\sigma_{nf}(^{235}U)$ ratios and their error levels

E, MeV	$\frac{\sigma_{nf}(^{244}Cm)}{\sigma_{nf}(^{235}U)}$	$\Delta\frac{\sigma_{nf}(^{244}Cm)}{\sigma_{nf}(^{235}U)}$,%	E, MeV	$\frac{\sigma_{nf}(^{244}Cm)}{\sigma_{nf}(^{235}U)}$	$\Delta\frac{\sigma_{nf}(^{244}Cm)}{\sigma_{nf}(^{235}U)}$,%
			1,5	1,511	
			1,6	1,475	
			1,8	1,421	
			2,0	1,412	
			2,4	1,448	7
0,10	0,037	50	2,8	1,506	
0,12	0,036		3,2	1,556	
0,14	0,036		3,6	1,594	
0,16	0,037		4,0	1,630	
0,20	0,040		4,5	1,647	
0,25	0,055		5,0	1,706	10
0,30	0,080	30	5,5	1,760	
0,35	0,117		6,0	1,826	
0,40	0,171		6,5	1,672	
0,45	0,259		7,0	1,574	
0,50	0,379	10	8,0	1,387	
0,55	0,521		9,0	1,380	
0,60	0,719		10	1,384	10
0,65	0,911		11	1,383	
0,7	1,113	7	12	1,356	
0,75	1,277		13	1,227	
0,8	1,415		14	1,123	
1,0	1,632	5	15	1,120	10
1,1	1,661		16	1,158	
1,2	1,637		17	1,220	
1,3	1,597		18	1,250	
1,4	1,558		19	1,245	
			20	1,181	10

Therefore, the evaluation is based on calculations using theoretical models and systematics.

4.1. Optical cross-sections

Optical cross-sections and neutron transmission coefficients were calculated using the coupled channels method and the COUPLE program [29] with the potential parameters from Ref. [30]. The quadrupole β_2 and hexadecapole β_4 deformation parameters for ^{244}Cm were obtained using the β_2 and β_4 dependence, which may be predicted with some accuracy by means of microscopic calculations, and the values for the latter selected for ^{238}U in Ref. [30]. The quadrupole deformation parameter β_2 was then fine tuned by

fitting the calculated value of the strength function S_0 to the evaluated value for the resolved resonance region.

$$V_R = 46{,}1-0{,}3\cdot E, \quad r_R = 1{,}256, \quad a_R = 0{,}626;$$

$$W_D = \begin{cases} 3{,}1+0{,}4\cdot E, & E \leq 10 \text{ МэВ}, \quad r_D = 1{,}260, \\ 7{,}1, & E > 10 \text{ МэВ}, \quad a_D = 0{,}555+0{,}0045\cdot E; \end{cases}$$

$$V_{so} = 7{,}5, \quad \beta_2 = 0{,}230, \quad \beta_4 = 0{,}020.$$

The calculations took into account the connection between the first three levels of the main rotational band of ^{244}Cm (see Table 2).

4.2. Values calculated using a statistical model

The cross-sections of processes occurring after formation of the compound nucleus were calculated using a statistical model. In the target nucleus discrete levels region, we employed Hauser-Feshbach-Moldauer formalism in our calculations; above that region we used the formalism of Tepel et al. The level density in the neutron and fission channels was determined using the functions of the superfluid model from Ref. [31], which was neatly fitted together with the constant temperature model in the lower region, and the systematics parameters from Ref. [32]. The radiative capture transmission coefficients were calculated using the gamma ray cascade emission model with the absorption curve parameters from Ref. [32], normalizing the radiative capture width to the evaluated value $\langle\Gamma_\gamma\rangle$ = 36 MeV. The cross-sections of reactions with preliminary emission of neutrons (n,n'x) were obtained by calculation using the STAPRE program [33]. Tables 4.1 and 4.2 give the evaluated cross-sections for interaction of neutrons with the ^{244}Cm nucleus in the 0.045-20 MeV fast neutron region.

Comparing the evaluated ^{244}Cm cross-sections with the data in ENDF/B-V [28], we see (Fig. 4.1) that the differences are due to the different theoretical models used to predict the cross-sections. In the evaluation in Ref. [28], the cross-sections in the fast neutron region were obtained via calculations based on a spherical optical model and a statistical model which did not take into account pre-equilibrium emission of neutrons. The biggest differences are in the cross-sections for excitation of discrete levels, the total inelastic scattering cross-section, and the (n,2n) and (n,3n) reaction cross-sections.

Table 4.1

Evaluated data on ^{244}Cm neutron cross-sections in the fast neutron region, 10^{-28} m^2

E, MeV	σ_t	σ_{nn}	σ_{nf}	$\sigma_{n\gamma}$	$\sigma_{nn'}$	σ_{n2n}	σ_{n3n}
1	2	3	4	5	6	7	8
0,043	14,752	13,783	0,071	0,898	-		
0,045	14,412	13,454	0,069	0,865	0,024		
0,050	14,287	13,324	0,068	0,778	0,117		
0,06	14,066	13,039	0,065	0,650	0,312		
0,07	13,871	12,770	0,062	0,562	0,477		
0,08	13,692	12,523	0,060	0,499	0,610		
0,10	13,362	12,055	0,058	0,432	0,817		
0,12	13,058	11,657	0,055	0,384	0,963		
0,14	12,770	11,297	0,053	0,352	1,068		
0,16	12,512	10,983	0,053	0,329	1,147		
0,20	12,034	10,423	0,055	0,302	1,254		
0,25	11,514	9,818	0,071	0,279	1,346		
0,30	11,033	9,283	0,101	0,267	1,382		
0,35	10,599	8,790	0,145	0,263	1,401		
0,40	10,211	8,333	0,207	0,261	1,410		
0,45	9,862	7,894	0,307	0,255	1,406		
0,5	9,554	7,469	0,442	0,247	1,396		
0,55	9,277	7,068	0,602	0,235	1,372		
0,6	9,031	6,647	0,823	0,214	1,347		
0,65	8,812	6,252	1,039	0,194	1,327		
0,7	8,620	5,853	1,266	0,175	1,326		
0,75	8,450	5,515	1,452	0,162	1,321		
0,8	8,300	5,236	1,612	0,153	1,299		
0,9	8,057	4,788	1,847	0,137	1,285		
1,0	7,860	4,426	1,991	0,126	1,317		
1,1	7,741	4,196	2,018	0,123	1,404		
1,2	7,644	4,026	1,997	0,119	1,502		
1,3	7,577	3,878	1,969	0,117	1,613		
1,4	7,543	3,807	1,930	0,114	1,692		
1,5	7,519	3,749	1,892	0,111	1,767		
1,6	7,509	3,707	1,864	0,109	1,829		
1,8	7,520	3,679	1,830	0,105	1,906		
2,0	7,557	3,703	1,833	0,101	1,920		
2,4	7,653	3,837	1,850	0,090	1,876		
2,8	7,726	3,996	1,867	0,073	1,790		
3,2	7,780	4,118	1,869	0,048	1,745		
3,6	7,774	4,184	1,857	0,029	1,704		
4,0	7,732	4,195	1,845	0,017	1,675		
4,5	7,630	4,141	1,830	0,014	1,645		
5,0	7,490	4,030	1,815	0,011	1,634		
5,5	7,324	3,882	1,832	0,009	1,601		
6,0	7,140	3,714	2,031	0,008	1,387		
6,5	6,946	3,538	2,281	0,008	1,119	0	
7,0	5,751	3,366	2,445	0,007	0,924	0,009	
8,0	6,425	3,063	2,472	0,006	0,668	0,216	
9	6,176	2,840	2,445	0,005	0,557	0,329	
10	6,021	2,705	2,420	0,004	0,508	0,384	
11	5,912	2,645	2,395	0,003	0,476	0,393	
12	5,920	2,655	2,370	0,002	0,467	0,426	0
13	5,934	2,718	2,350	0,001	0,440	0,424	0,001
14	5,981	2,819	2,322	0,001	0,416	0,368	0,055
15	6,114	2,943	2,356	0,001	0,417	0,290	0,107
16	6,210	3,074	2,394	0,001	0,374	0,231	0,136
17	6,333	3,204	2,422	0,001	0,357	0,191	0,158
18	6,428	3,322	2,423	0,001	0,345	0,161	0,176
19	6,509	3,422	2,427	0,001	0,323	0,142	0,194
20	6,568	3,501	2,436	0,001	0,307	0,125	0,198

Table 4.2

Evaluated level excitation cross-sections for ^{244}Cm, 10^{-28} m^2

E, MeV	Level energy, keV					Excitation of continuous spectrum
	42,9	142,3	42,9	142,3	296	
	Direct excitation		Compound nucleus mechanism			
I	2	3	4	5	6	7
0,045	-	-	0,024			
0,05	0,001		0,116			
0,06	0,002		0,310			
0,07	0,004		0,473			
0,08	0,006		0,604			
0,10	0,011		0,806			
0,12	0,017		0,946			
0,14	0,023		1,045			
0,16	0,029		1,118	-		
0,20	0,043	-	1,209	0,002		
0,25	0,060	0,001	1,269	0,016		
0,30	0,078	0,002	1,273	0,029		
0,35	0,096	0,004	1,254	0,017		
0,40	0,115	0,007	1,220	0,068		
0,45	0,134	0,011	1,169	0,092		
0,50	0,153	0,016	1,109	0,118		
0,55	0,173	0,021	1,030	0,147	0,001	-
0,60	0,193	0,027	0,940	0,180	0,002	0,005
0,65	0,212	0,033	0,844	0,198	0,003	0,037
0,70	0,232	0,040	0,727	0,206	0,004	0,117
0,75	0,251	0,047	0,647	0,209	0,006	0,161
0,8	0,269	0,054	0,576	0,209	0,007	0,184
0,9	0,304	0,068	0,470	0,205	0,012	0,226
1,0	0,344	0,083	0,384	0,200	0,016	0,290
1,1	0,365	0,095	0,330	0,195	0,020	0,399
1,2	0,391	0,106	0,301	0,191	0,026	0,487
1,3	0,414	0,116	0,276	0,186	0,030	0,591
1,4	0,434	0,125	0,273	0,184	0,035	0,641
1,5	0,451	0,132	0,252	0,178	0,037	0,717
1,6	0,466	0,138	0,241	0,171	0,039	0,774
1,8	0,486	0,146	0,182	0,135	0,035	0,922
2,0	0,498	0,150	0,131	0,100	0,027	1,014
2,4	0,499	0,151	0,059	0,046	0,015	1,106
2,8	0,485	0,148	0,022	0,019	0,006	1,111
3,2	0,466	0,145	0,008	0,007	0,003	1,116
3,6	0,446	0,139	0,003	0,003	0,001	1,112
4,0	0,427	0,133	0,001	0,001	-	1,113
4,5	0,405	0,124	-	-		1,116
5,0	0,386	0,116				1,132
5,5	0,370	0,108				1,123
6,0	0,356	0,100				0,931
6,5	0,343	0,093				0,683
7,0	0,330	0,087				0,507
8,0	0,306	0,078				0,284
9,0	0,284	0,069				0,204
10	0,267	0,066				0,175
11	0,268	0,063				0,145
12	0,266	0,070				0,131
13	0,261	0,072				0,107
14	0,253	0,071				0,092
15	0,245	0,089				0,083
16	0,236	0,062				0,076
17	0,228	0,063				0,066
18	0,220	0,067				0,058
19	0,213	0,058				0,052
20	0,206	0,054				0,047

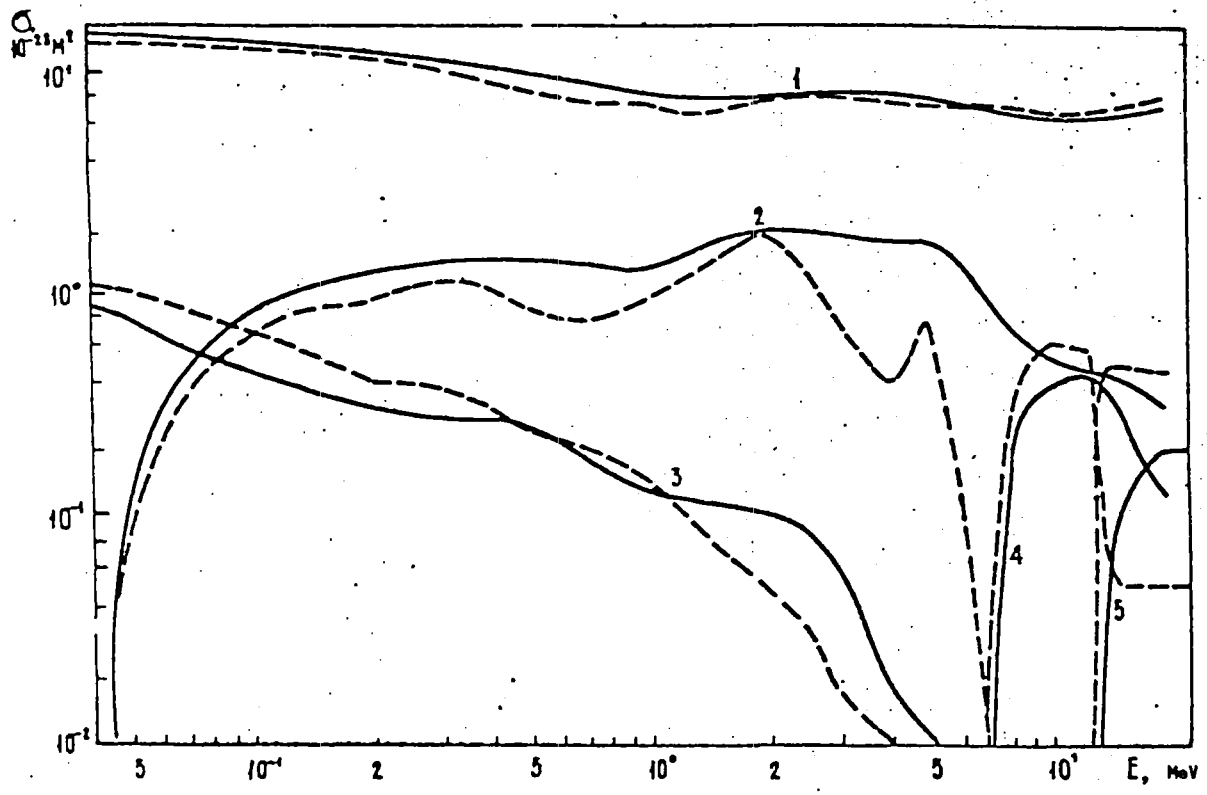

Fig. 4.1 Comparison of evaluated ^{244}Cm cross-sections in the fast neutron region: 1 - σ_t; 2 - $\sigma_{n,n'}$; 3 - $\sigma_{n\gamma}$; 4 - $\sigma_{n,2n}$; 5 - $\sigma_{n,3n}$; ----- - our evaluation; - - - - Evaluation in ENDF/B-V [28]

5. EVALUATION OF THE CHARACTERISTICS OF SECONDARY NEUTRONS AND THE $\bar{\nu}$ VALUE FOR ^{244}Cm

No experimental data are available on the energy and angular distributions of secondary neutrons and the $\bar{\nu}$ value for ^{244}Cm, and our evaluation was therefore based on known systematics and theoretical calculations.

The angular neutron distributions for the elastic and inelastic scattering reactions at the first two levels were presented as decomposition values using Legendre polynomials. These values were calculated using the generalized optical model taking into account the isotropic addition from the part of these processes occurring after the compound nucleus stage. The angular distributions of neutrons emitted in the remaining reactions ere assumed to be isotropic. The energy distributions of secondary neutrons were calculated using a statistical model which took into account possible pre-equilibrium emission of neutrons. This method is described in detail in Ref. [31].

The mean number of prompt fission neutron $\bar{\nu}_p$ was calculated using Howerton's methodology [32], experimental data on fission thresholds, our evaluation values for

$$R_x(E) = \frac{\sigma_{n,xnf}}{\sigma_{nF}}, \quad x = 0, 1, 2$$

and the mean energies of pre-fission neutrons emitted in the (n,n'f) and (n,2nf) reactions. The mean number of delayed fission neutrons and its energy dependence were selected using the systematics from Ref. [35] which predict the dependence of $\bar{\nu}_d$ on the parameter A-3Z: $\bar{\nu}_d$ = 0. 047 (E = 10^{-5} -5 MeV); $\bar{\nu}_d$ = 0.030 (E = 9-20 MeV). In the 5-9 MeV interval, the reduction in ν_d from 0.047 to 0.030 is linear. The evaluated values of $\bar{\nu}_p$ and $\bar{\nu}_t = \bar{\nu}p_p + \bar{\nu}_d$ are given in Table 5.1.

The fission neutron spectrum is given in the form of the Maxwell distribution. The temperature of this spectrum T_M for fission of ^{244}Cm by thermal neutrons was obtained from experimental data on the mean energy of fission spectra $\bar{E} \sim 3/2\ T_M$ for other nuclei, assuming that $\bar{E}$ is a linear

Table 5.1

Mean number of neutrons emitted per fission event

E, MeV	$\bar{\nu}_p$	$\bar{\nu}_t$	E, MeV	$\bar{\nu}_p$	$\bar{\nu}_t$
10^{-5}	3,105	3,152	12,0	5,140	5,170
1,0	3,289	3,336	15	5,600	5,630
5,0	4,025	4,072	18	6,013	6,043
6,0	4,191	4,234	20	6,288	6,318
9,0	4,655	4,685			

function of the parameter Z^2/A. The energy dependence of T_M was given in the form

$$T_M(E) = a + b\,[1 + \bar{\nu}(E)]^{1/2},$$

where

$$\bar{\nu}(E) = [\bar{\nu}_t(E)\sigma_{nF}(E) - \sigma_{n,n'f}(E) - 2\,\sigma_{n,2nf}(E)]/\sigma_{nF}(E),$$

and the parameters a = 0.971 and b = 0.242 were selected in such a way that

they agreed with the value of T_M at the thermal point, and described the ~ 1% rise in T_M for a 1 MeV increase in excitation energy.

CONCLUSION

As mentioned above, owing to its high α-activity and the difficulty of preparing pure targets, experimental data on the cross-sections for interaction of neutrons with the ^{244}Cm nucleus are very limited in extent. Therefore, this evaluation has made wide use of various theoretical models, and the accuracy of the evaluated data is directly related to their reliability. The appearance of new experimental data on ^{244}Cm may significantly improve upon our evaluation.

REFERENCES

[1] IGARASI, S., NAKAGAWA, T., "Requirements and status of transactinium isotope nuclear reactor data", Transactinium Isotope Nuclear Data - 1984, IAEA-TECDOC-336, IAEA, Vienna (1985) 57-104.

[2] LEDERER, C.M., SHIRLEY, V.S., Tables of Isotopes, 7 Ed., J. Whiley and Sons, Inc., New York (1978);

[3] COTE, R.E., BARNES, R.F., DIAMOND, H., Total neutron cross-sections of ^{244}Cm, Phys. Rev., 134 6B (1964) 1281-1284.

[4] BERRETH, J.R., SIMPSON, F.B., RUSCHE, B.C., The total neutron cross-sections of the curium isotopes from 0.01 to 30 eV, NSE 49 (1972) 145-152.

[5] SIMPSON, O.D., SIMPSON, F.B., YOUNG, T.E., et al., "An analysis and evaluation of the ^{244}Cm total, capture and fission cross-sections below 530 eV", Report USNDC-3 (1972) 4-7.

[6] MOORE, M.S., KEYWORTH, G.A., Analysis of the fission and capture cross-sections of the curium isotopes, Phys. Rev., C 3 4 (1971) 1656-1667.

[7] BELANOVA, T.S., KOLESOV, A.G., PORUCHIKOV, V.A., et al., "Neutron resonance parameters of the curium isotopes", Neutron Physics, TsNIIatominform, Moscow (1977) 260-262 [in Russian].

[8] MAGUIRE, H.T., STOPA, C.R., BLOCK, R.C., et al., Neutron induced fission cross-section measurements of ^{244}Cm, ^{246}Cm and ^{248}Cm, NSE 89 4 (1985) 293-304.

[9] STEVENS, C.M., STUDIER, M.H., FIELDS, P.R., et al., Curium isotopes 246 and 247 from pile-irradiated plutonium, Phys. Rev., 94 4 (1954) 974.

[10] KROSHKIN, N.I., ZAMYATNIN, Yu.S., Measurement of energy spectra and the mean number of $\bar{\nu}$ of prompt fission neutrons, At. Ehnerg. 29 2 (1970) 95-98 [in Russian].

[11] SCHUMAN, R.P., "Resonance integrals from the cadmium shielded irradiation of ^{244}Cm", Report WASH-1136 (1970) 54-55.

[12] THOMPSON, M.S., HYDER, M.L., RUCLAND, R.J., Thermal neutron cross-sections and resonance integrals for ^{244}Cm through ^{248}Cm, Journal of Inorg. and Nucl. Chemistry, 33 6 (1971) 1553-1560.

[13] BENJAMIN, R.W., MACMURDO, K.W., SPENCER, J.D., Fission cross-sections for five isotopes of curium and californium-249, NSE 47 (1972) 203-208.

[14] ZHURAVLEV, K.D., KROSHKIN, N.I., CHETVERIKOV, A.P., Cross-sections and resonance integrals for fission of ^{239}Pu, ^{249}Cf and Am and Cm isotopes, At. Ehnerg. 39 4 (1975) 285-286 [in Russian].

[15] GAVRILOV, V.D., GONCHAROV, V.A., Thermal cross-sections and resonance integrals for capture of neutrons by $^{244-248}$Cm and ^{250}Cf nuclei, At. Ehnerg. 44 3 (1978) 246-247 [in Russian].

[16] FOURHIER, J.M., BLAISE, A., MULLER, W., SPIRLET, J.C., Curium: a new magnetic element, Physica (Utrecht) 86-88 (B + C) (1977) 30.

[17] PORODZINSKIJ, Yu.V., SUKHOVITSKIJ, E.Sh., Method for determining mean neutron widths and inter-level distances taking into account the finite resolution of experimental apparatus, Vestsi AN BSSR, Ser, Fiz.,-Ehnerg. Navuk. 3 (1986) 19-23 [in Russian].

[18] FULLWOOD, R.R., MCNALLY, J.H., SHUNK, E.R., "Neutron induced fission cross-section measurements in ^{244}Cm", Neutron Cross Sections and Technology (Proc. COnf., Washington, 1968), Vol. 1, 567-572.

[19] FOMUSHKIN, Eh.F., NOVOSELOV, G.F., VINOGRADOV, Yu.I., et al., Cross-sections for neutron-induced fission of ^{244}Cm and ^{246}Cm in the vicinity of the threshold, Yad. Fiz. 31 1 (1980) 39-42 [in Russian].

[20] Measurement of the effective cross-sections for fast reactor neutron-induced fission of the isotopes $^{244-248}$Cm, Yad. Fiz. 17 1 (1973) 24-27 [in Russian].

[21] KOONTZ, P.D., BARTON, D.M., "Techniques for fission cross-section measurements for elements with high α- and spontaneous fission activity", Neutron Cross Sections and Technology (Proc. Conf., Washington, 1968), Vol. 1, 597-602.

[22] VOROTNIKOV, P.E., KOZLOV, L.D., MOLCHANOV, Yu.D., Measurement of the cross-section for fast neutron-induced fission of ^{244}Cm using a nanogram quantity of the isotope, At. Ehnerg. 57 1 (1984) 61-62 [in Russian].

[23] FOMUSHKIN, Eh.F., GUTNIKOVA, E.K., ZAMYATIN, Yu.S., et al., Cross-sections and angular fragment anisotropy in fast neutron-induced fission of certain isotopes of plutonium, americium and curium, Yad. Fiz. 5 (1967) 966-970 [in Russian].

[24] VANKOV, G.B., "The ^{235}U fission cross-section", Nuclear Data Standards for Nuclear Measurements, Techn. Rep. Series No 227, Vienna (1983) p. 39-45.

[25] SMITH, A.B., "The ^{235}U fission cross-section", Nuclear Data Standards for Nuclear Measurements, Techn. Rep. Series No. 227, Vienna (1983) 53-57.

[26] GRUDZEVICH, O.T., IGNATYUK, A.V., MASLOV, V.M., PASHCHENKO, A.B., "Co-ordinated description of the (n,n'f) and (n,xn) reaction cross-sections for transuranium nuclei", Neutron Physics (Proc. Sixth All-Union Conf., Kiev, 2-6 October, 1983), Vol. 2, TsNIIatominform, Moscow (1983) 318-323 [in Russian].

[27] BRITT, H.C., WILHELMY, Y.B., Simulated (n,f) cross-sections for exotic actinide nuclei, NSE 72 (1979) 222-229.

[28] KINSEY, R., ENDF/B Summary Documentation, BNL-17541 (ENDF-201) Brookhaven (1979).

[29] KLEPATSKIJ, A.B., KON'SHIN, V.A., SUKHOVITSKIJ, E.Sh., The coupled channels method and evaluation of neutron data for fissile nuclei, Vestsi AN BSSR Ser. Fiz.-Ehnerg. Navuk. 2 (1984) 21-29 [in Russian].

[30] KLEPATSKIJ, A.B., KON'SHIN, V.A., SUKHOVITSKIJ, E.Sh., Optical potential for heavy nuclei, Vopr. Atom. Nauki i Tekhniki, Ser. Yad. Konstanty 1 (45) (1982) 29-33 [in Russian].

[31] KLEPATSKIJ, A.B., KON'SHIN, V.A., MASLOV, V.M., et al., Evaluated Neutron Constants for Uranium-236, Preprint IYaEh AN BSSR [Nuclear Power Institute of the Academy of Sciences of the Byelorussian SSR], No. 2, Minsk (1987) 83 [in Russian].

[32] ANTSIPOV, G.V., KON'SHIN, V.A., MASLOV, M.V., Level density and radiation widths of the transactinides, Vopr. Atom. Nauki i Tekhniki, Ser. Yad. Konstanty 3 (1985) 25-34 [in Russian].

[33] UHL, M., STROHMAIER, B., Report IRK76/01, Vienna (1976).

[34] HOWERTON, R.M., $\bar{\nu}$ revisited, NSE 62 (1977) 438-454.

[35] MANERO, F., KON'SHIN, V.A., Status of the energy-dependent $\bar{\nu}$-values for the heavy isotopes (Z > 90) from thermal to 15 MeV and $\bar{\nu}$-values for spontaneous fission, At. Energy Rev. 10 4 (1972) 637-756.